Journal of Colloid and Interface Science 663 (2024) 458–466

Contents lists available at ScienceDirect

Journal of Colloid And Interface Science

journal homepage: www.elsevier.com/locate/jcis

Regular Article

The significance of multipole interactions for the stability of regular structures composed from charged particles

Eric B. Lindgren [a], Holly Avis [b], Abigail Miller [b], Benjamin Stamm [a], Elena Besley [b], Anthony J. Stace [b,*]

[a] Institute of Applied Analysis and Numerical Simulation, University of Stuttgart, Pfaffenwaldring 57, 70569 Stuttgart, Germany
[b] School of Chemistry, University of Nottingham, University Park, Nottingham NG7 2RD, United Kingdom

HIGHLIGHTS

- Application of new theory to the treatment of many-body interactions between charged, dielectric particles.
- Study of six particle lattice stoichiometries, AB, AB_2, AB_3, AB_4, AB_5 and AB_6.
- Calculations reveal the significance dielectric constant has for the stabilities of certain lattice types.
- A new lattice isostructural with CFe_4 is found to be particularly stable due to many-body effects.

GRAPHICAL ABSTRACT

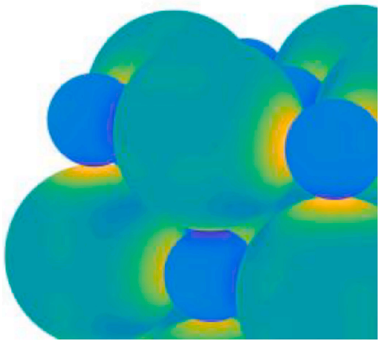

ARTICLE INFO

Keywords:
Charged particles
Many-body effects
Dielectric constant
Binary particle lattices

ABSTRACT

Identifying the forces responsible for stabilising binary particle lattices is key to the controlled fabrication of many new materials. Experiments have shown that the presence of charge can be integral to the formation of ordered arrays; however, a complete analysis of the forces responsible has not included many of the significant lattice types that may form during fabrication. A theory of many-body electrostatic interactions has been applied to six lattice stoichiometries, AB, AB_2, AB_3, AB_4, AB_5 and AB_6, to show that induced multipole interactions can make a very significant (>80 %) contribution to the total lattice energy of arrays of charged particles. Particle radii ratios which favour global minima in electrostatic energy are found to be the same or a close match to those observed by experiment. Although certain lattice types exhibit local energy minima, the calculations show that many-body rather than two-body interactions are ultimately responsible for the structures observed by experiment. For a lattice isostructural with CFe_4, a particle size ratio not previously observed is found to be particularly stable due to many-body effects.

* Corresponding author.
E-mail address: Anthony.stace@nottingham.ac.uk (A.J. Stace).

https://doi.org/10.1016/j.jcis.2024.02.146
Received 27 October 2023; Received in revised form 25 January 2024; Accepted 19 February 2024
Available online 22 February 2024

1. Introduction

There are numerous examples throughout nature of where the presence of charge on a particle is considered to make an important contribution to the process of coalescence or aggregation. For example, the tribocharging of sand particles have been linked to sediment transport and aggregation on Titan [1], and the coagulation of charged dust particles has been proposed as a mechanism for the formation of protoplanets [2,3]. These ideas are supported by laboratory experiments where, for example, Lee *et al.* have provided images that show step-by-step mechanisms where charged particles suspended in vacuum can coalesce via orbiting encounters [4]. Closer to home, the tribocharging of silicate dust and the resultant charged particle interactions has been proposed as a mechanism for the appearance of lightning during volcanic eruptions [5].

From the perspective of controlled assembly, it is recognised that the coalescence of charged particles into ordered arrays could be significant for the fabrication of new and novel devices [6]. The parameters available for fabricating binary arrays of particles are primarily relative size, composition (metal, semiconductor, insulator), stoichiometry and the nature of the interaction potential. Achieving precise control over the structure and morphology of any *ordered* two-particle array requires a complete understanding of the forces responsible for creating stability through long-range order; only then should it be possible to design new materials. Laboratory experiments by Whitesides and co-workers have shown that two-dimensional ordered arrays can be fabricated from mm-sized Teflon and Nylon particles that have acquired charge (negative and positive) from contact electrification [7,8]. Depending on particle composition and experimental conditions, captured images show the evolution of regular square, pentagonal and hexagonal arrays [7,8]. More recently computer simulations using many-body electrostatic theory have been successful in reproducing many of the observed patterns, which included chain configurations adopted to minimise the effects of excess charge [9]. These experiments on mm-sized charged polymer particles have since been extended into three dimensions by Haeberle *et al.* [10], who have shown that regular, 3 -dimensional closed-packed and body-centered cubic lattice structures can form in a container if the effects of gravity are minimised. The above experiments and calculations have involved particles with considerable variations in size, composition, and charge. Composition is significant because it determines the polarizability of a particle, which in turn determines its susceptibility to the presence of an external electric field. At a macroscopic level, polarizability is best measured by the magnitude of the dielectric constant of a particle, which for those materials referenced above ranges from ~2 for Teflon to ~15 for metal oxides.

Here, six of the most frequently observed binary particle stoichiometries [11–13] have been explored as a function of particle size ratio, γ, and the results used to furnish a quantitative discussion as to the importance of induced electrostatic interactions in determining the stabilities of regular structures and appropriate particle combinations. The calculations identify individual contributions from Coulombic and induced multipolar interactions and the results show that the latter can play a significant role in determining both structural stability and configurations with global minima [14]. Previous attempts to quantify the stabilities of AB_n lattices have mostly utilized pair potentials in the form of a van der Waals interaction together with either a screened Yukawa potential [15–19] or an unscreened point charge Coulomb potential [12,13]. The latter calculations incorporated the Madelung constant, which for a NaCl-like cubic lattice has a value of 1.7476, when charges of +e and −e reside on adjacent sites. The value for the Madelung constant varies according to lattice structure and the magnitude of charge, and earlier calculations [14] have shown that an arbitrary assignment of the constant is not necessary for each lattice type because its value can be accurately reproduced through a Coulomb and induced multipole treatment.

The purpose of the results presented here is to show how important many-body electrostatic interactions between polarisable dielectric particles are for the stabilities of ordered arrays, both those described above and those that could become important in future particle assemblies. Many-body interactions between polarizable spheres have been the subject of previous theoretical work [20–24]. Barros *et al.* [20,21] have used a surface-charge model to analyse the influence inhomogeneous surface charge distributions have on an assembly of polarisable colloid particles and point charges. They show, for example, that such an assembly can be sensitive to the nature of the dielectric constant, and where a change in value can induce a switch from an NaCl-type structure to a chain-like geometry [21]. Qin *et al.* have combined a scattering formalism with image charge methods to analyse the behaviour of collections of dielectric spheres in a NaCl-type lattice [22–24]; the calculations show the significance of multipolar interactions for the stability of this type of lattice.

In the work presented here a recent development in the theory of many-body electrostatic interactions [14] has been used to systematically examine six separate binary, dielectric particle stoichiometries, AB, AB_2, AB_3, AB_4, AB_5 and AB_6. The objective being to show the importance many-body interactions are for the stability of a range of lattice structures composed from charged particles. Altogether, nine separate lattice types are examined, where the significance of many-body interactions to structural stability is found to range from <20 % to >80 %.

2. Theory

A general solution based on an integral equation approach to the problem of calculating electrostatic interactions between large numbers of dielectric, spherical particles has previously been presented by Lindgren *et al.* [14] and shown to have a guaranteed error bound [25–27]. The solution provides an accurate, quantitative description of the problem, with a significant feature being that it is computationally very efficient, to the point where it has provided a force field for the simulation of charged particle dynamics [9]. In this work, static structures composed from arrays of charged particles with a range of stoichiometries are examined with a view to identify the significance particle polarizability has on the stability of regular structures.

The solution treats a number, M, of particles of arbitrary size, charge, dielectric constant, and position in three-dimensional space, embedded in a homogeneous medium of arbitrary dielectric constant. The system to be studied consists of a collection of M non-over lapping charged dielectric spheres, $\Omega_1, \ldots, \Omega_M$, which are suspended in three-dimensional space. Each particle Ω_i ($i = 1, 2, \ldots, M$) has a radius r_i, a position x_i ($i = 0, 1, \ldots, M$), and a dielectric constant $k_i \geq 1$. The spherical particles are described as uniform, solid balls ($\{\Omega_i\}_{i=1}^{M}$) with surfaces ($\{\Gamma_i\}_{i=1}^{M}$) and where the latter defines a boundary interface, $\Gamma_i = \partial\Omega_i$ between the interior, Ω^-, and the exterior, Ω^+, of the particles. All particles are suspended in a homogeneous medium of dielectric constant k_0, where in the present case $k_0 = 1$for air or vacuum.

Each particle carries a free charge q_i, uniformly distributed over the surface and is represented by a surface density, $\sigma_{f,i} = q_i/(4\pi r_i^2)$ that is completely supported by the boundary Γ_i, such that a global function, $\sigma_f(x)$ can be defined as:

$$\sigma_f(x) = \begin{cases} \sigma_{f,i} \;\; at \;\; all \;\; boundaries \\ 0 \qquad \text{otherwise} \end{cases}$$

Accordingly, the presence of free charge, $\sigma_{f,i}$, on the particles gives rise to an electrical potential, Φ, at each point in the system, which is defined as a solution to:

$$-\nabla.(k\nabla\Phi) = 4\pi K\sigma_f \tag{1}$$

Where K is Coulomb's constant. If Φ can be determined, then the electrostatic potential energy, U, follows directly from [14]

$$U(\Phi, \sigma_f) = 2\pi K \int_{\Gamma_0} \sigma_f(s)\Phi(s)dx \quad (2)$$

where s denotes a point on the surface of a particle and $\Gamma_0 = \Gamma_1 \cup \ldots \cup \Gamma_M$.

To represent the problem in terms of integral equations, it can be reformulated as an interface problem where, as with the two-body problem [28], the potential Φ has to be determined in such a way that standard boundary conditions are observed; in particular:

$$\Delta\Phi = 0 \text{ in each } \Omega_i (i = 1, \cdots M),$$

$$[\![\Phi]\!] = 0 \text{ on } \Gamma_0,$$

$$[\![k\nabla\Phi]\!] = 4\pi K\sigma_f \text{ on } \Gamma_0$$

where $[\![\Phi]\!]$ and $[\![k\nabla\Phi]\!]$ denote the jump of Φ and $k\nabla\Phi$, respectively As presented elsewhere [14,25], an integral equation that uniquely represents Φ for a global charge density σ_f can be derived, and a solution obtained through a discretisation based on numerical integration in the space of truncated spherical harmonics. The resultant set of linear equations can be solved iteratively. The total electrostatic energy of the system can be obtained from Eq. (2) and the net electrostatic force on each particle, Ω_i, comes as the gradient of the energy with respect to changes in x_i (i = 0,1, …, M) [14,27]. Thus, the accuracy of each calculation is controlled through the maximum number, N, of real spherical harmonics utilised in discretisation of the model. This parameter has been set as $N = 6$ in all calculations, which as convergence test show [14], equates to an average error of 4 % in the multipole terms.

For examples that involve large numbers of particles, the evaluation of multipole interactions benefits from the implementation of a fast multipole method (FMM) [29], which provides a significant enhancement to the speed of computation, to the point where there is a linear scaling with respect to the number of particles and the time required for each computation of the force [14,26,27]. Hence, FMM reduces the number of calculations needed for each particle by creating a grid, where the charge of every particle within an individual cell in the grid is transformed to a single point multipole; a procedure that is repeated in a multi-scale manner. This means that any particle outside the neighbourhood of a corresponding cell only has to interact with a single point multipole instead of each and every particle inside a particular grid. This procedure drastically reduces the number of calculations required and makes the computation of large lattice structures tractable. FMM is highly technical, and a detailed discussion goes beyond the scope of this paper [29]. If FMM is not used, the complexity of a general three-dimensional particle configuration scales as the square of the number of particles instead of a linear scaling. Further, FMM scales as the third power of the degree of spherical harmonic utilised in the underlying expansions; without FMM, it scales as the fourth power.

In the examples that follow, Coulomb and charge-induced multipolar interactions are considered up to the sixth degree (N = 6, 64 pole), and where the non-additive nature of these interactions [30] is taken into account through the mutual polarisation of charged, dielectric particles (see Fig. 1). The model takes as input the number of particles, each with an assigned radius, dielectric constant (relative permittivity), charge and position in three-dimensional space. Output consists of the distribution of surface charge, the electrostatic energy and the total force acting on each particle. The charge that is assigned, denoted here as *free* charge, is the quantity over which experimentalists generally have control and is treated in the model as being fixed and uniformly distributed over the surface of each particle. However, as the particles are considered to be composed of a dielectric material, they become polarised when in the presence of an external electric field, which in this context is generated by the presence of free charge on adjacent particles. As a consequence, polarised bound charge accumulates on the surface of each particle, which leads to an anisotropic distribution of total (*free* + *bound*) surface charge. This is coupled with similar processes on all other particles via mutual polarisation; a mechanism which can only be properly described through a many-body formalism. Previous calculations have explored the effect charge inhomogeneity in the form of either negatively and positively charged patches or as localised point charges has on both the geometry and the strengths of particle–particle interactions [31,32].

In addition to enhancing charge-induced multipole interactions, there exists the possibility of a further effect due to the presence of polarisable particles, and that is like-charge attraction [28,33]. However, such behaviour requires particles with the same sign of charge to be in close proximity and will only arise if the size ratio is small and or the charge difference is large [33]. The complementary medium has

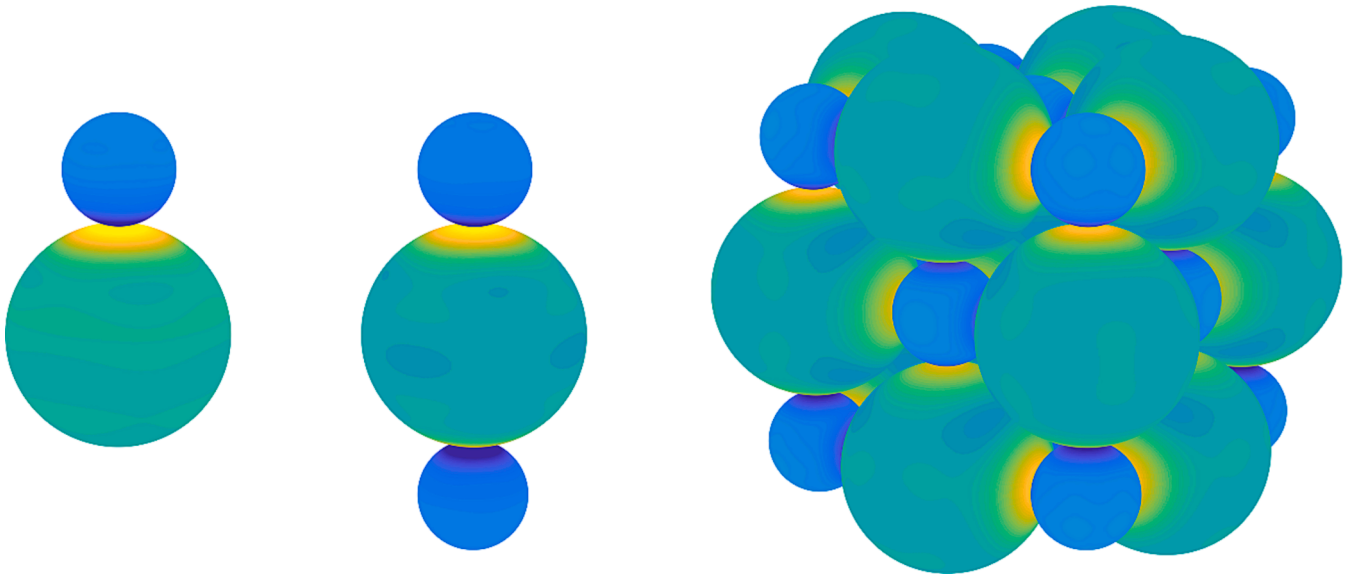

Fig. 1. Calculated surface charge on polarisable particles in a NaCl lattice configuration. Isolated two-body and three-body interactions are shown together with a larger section of the lattice. The yellow and dark blue features correspond to regions of increased positive and negative charge, respectively, where there is enhanced polarisation of bound charge towards the points of contact. In the many-body example, polarisation is polydirectional causing the polarised charge to concentrate at a number of sites on each particle. (For interpretation of the references to colour in this figure legend, the reader is referred to the web version of this article.)

been given a dielectric constant appropriate for a vacuum; however, the consequence of including a solvent in a many-body treatment has recently been addressed [23,34]. The effects of suspending polarisable particles in an electrolyte solution has also been investigated, and where it is shown that for calculated forces there are significant departures from DLVO theory when particles are in close proximity to one another [35]. The theory [14] has been developed for the purposes of investigating the behaviour of collections of charged particles; however, we note that similar developments in the theory of electrostatics have been presented by Lotan and Head-Gordon for the purposes of studying proteins [36].

Convergence tests has been performed to determine the most suitable size of lattice for the calculations; for all AB_n structures, each particle A was given a charge of $q_1 = +1$ and each particle B a charge of $q_2 = -1/n$ to ensure overall neutrality. For all the lattice types considered here, the total electrostatic energy per particle was found to have converged to within ≈ 0.4 % once the lattice contained 1000 particles, and all subsequent calculations have used that number of particles to give an appropriate balance between computational cost and accuracy. Previous calculations showed that for the example of an atomic NaCl lattice, where anion and cation spheres appropriate for the sizes of Na^+ and Cl^- were used, the lattice energy and the Madelung constant asymptotically approached their literature values as the number of charged particles increased [14].

3. Results and discussion

3.1. Lattice stoichiometries

The binary particle lattices chosen for this study cover a range of stoichiometries, which include AB, AB_2, AB_3, AB_4, AB_5 and AB_6, all of which have been observed in experiments, but have not necessarily involved the interaction of charged particles [11–13]. For each of these examples, the total electrostatic energy and the individual contributions of Coulomb and multipolar interaction energy, have been investigated as a function of the particle radius ratio $\gamma = r_{small}/r_{large}$, where r_{small} is the radius of the smaller particle and r_{large} is the radius of the larger particle. A dielectric constant of 20 for both particles has been used as a compromise between particles that are weakly polarisable, such as hydrocarbons and polymers, and particles that are strongly polarisable for example, water droplets (ice), metal oxides and metals. For the systems already identified above, dielectric constants range from $k_i = 4$ for nylon, through to $k_i \approx 15$ for ZrO_2 particles. However, the consequences of changing the dielectric constant are also examined. Starting structures for the binary lattices studied were based on particulate structures previously observed by experiment, and these are isostructural with NaCl, CsCl, CuAu, AlB_2, $MgZn_2$, $AuCu_3$, CFe_4, $CaCu_5$, CaB_6 [11–13,37]. Crystallographic Information Files (CIF), containing the coordinates of each of the above materials, have been downloaded from the Materials Project Database [38]. These dimensions have then been scaled up to an appropriate size using Avogadro and taken as starting conditions of each lattice type [39]. In all the examples, particle A refers to the first particle of each lattice type, B refers to the second particle, and *n* refers to the stoichiometry.

As an illustration of the consequences of including polarisation interactions, Fig. 1 gives a visual representation of the elements of an NaCl lattice type with a particle size ratio of 0.41, which is optimum for the packing of this particular lattice. In addition to the light blue and green colours representing the assigned free charges, there are also regions of enhanced positive and negative surface charge denoting the presence of bound charge that has been polarised by the close proximity of oppositely charged particles. A similar image for a colloidal lattice with an NaCl structure has been presented by Barros *et al.* [21], but with embedded point charges; in contrast, Fig. 1 shows the consequence of an interaction between charged, polarisable, dielectric particles.

3.2. Variation in particle size

The calculation of the interaction energies has been undertaken as a function of the radius ratio, γ, of particles A and B. Since the experimental literature on particle lattices covers charges ranging from ~0 ± 1e to 10^6e [4,7,8,11–13] and particle sizes that range from nanometres up to micrometres [4,7,8,11–13], both particles were assigned arbitrary values that fell within these extremes. For a formula unit AB_n the charge on particle A, q_1, was fixed at +1000 *e*, while the sum of the charges on each particle B was −1000 *e*, such that $q_2 = -1000/n$ *e*, thus ensuring overall neutrality. Both A and B particles ranged in radius from 50 μm to 500 μm, with the pivot point of each calculation corresponding to the size ratio $\gamma = 1$.

Fig. 2 shows the total electrostatic energy as a function of γ calculated for particle combinations that identify with each of the crystallographic structures NaCl, CsCl, CuAu, AlB_2, $MgZn_2$, $AuCu_3$, CFe_4, $CaCu_5$ and CaB_6.

As might be expected, all three of the AB lattice types show two minima depending on whether either A or B is the smaller of the two particles; and within this group, the NaCl lattice is by far the most stable. Of the remaining lattices, only that with a CFe_4 configuration has a minimum where A (C) is the smaller particle; this lattice also has a second, poorly defined minimum, where B (Fe) is very small. Two lattice types, $AuCu_3$ and $CaCu_5$, exhibit two minima as a function of γ, where those associated with $AuCu_3$ coincide with experimental observations, whereas there is a discrepancy between calculation and observation for $CaCu_5$ [11]. A second minimum for $AuCu_3$ is more evident in Fig. 5 below. These results are summerised in Table 1, together with relevant experimental data that have been determined from the packing of particles [11,12,37]; however, these latter results are not necessarily the product of interactions between *charged* particles. As can be seen, there is very good agreement between the calculated and experimental results, with the only notable discrepancy being $CaCu_5$; however, the experimental result does fall within the two calculated minima.

As part of the calculations, the total energies shown in Fig. 2 have been broken down into individual contributions arising from Coulomb and many-body polarisation interactions. Whilst the former can be either attractive or repulsive, polarisation interactions between charged particles in vacuum are always attractive, and can in some instances, be responsible for the presence of like-charge attraction [28]. However, calculations have shown that changes in the dielectric constant ratio, $k_{particle}/k_{medium}$ can introduce repulsive interactions [23,40]. Fig. 3 show the calculated Coulomb energy for each of the lattice types as a function of γ. Here there are several interesting features; first, it is obvious that none of the lattices exhibit distinct minima at kinks (discontinuities in the derivative) in the Coulomb energy. For example, as the particle size ratio is reduced, the NaCl lattice shows a kink at $\gamma = 0.42$, but below that point the Coulomb energy remains constant. Similar behaviour is seen for all the other lattice types, apart from CFe_4, which exhibits no discontinuities and has more or less constant Coulomb energy across the entire range of γ. Secondly, the CaB_6 lattice is calculated to be electrostatically unstable if just the *Coulomb* energy is taken into consideration, and where at a value of $\gamma = 0.4$, which is calculated to be a minimum in the *total energy*, there is a distinct increase in the Coulomb energy. Two other lattice types, CFe_4 and AlB_2, are also close to being unstable in terms of just their Coulomb energy.

The reason why lattices exhibit a constant Coulomb energy below certain radius ratios can be illustrated with the NaCl lattice. As seen in Fig. 4, when the radius ratio drops below 0.41 for this type of geometry, each large particle is now in contact with the next nearest large particle (as defined in terms of a three-dimensional structure); hence displacement of their centres with any further decrease in the value of γ becomes constrained. Therefore, to maintain fixed lattice positions, radius ratios below 0.41 can only be achieved by changing the relative sizes of the particles.

A uniform distribution of charge is electrostatically equivalent to

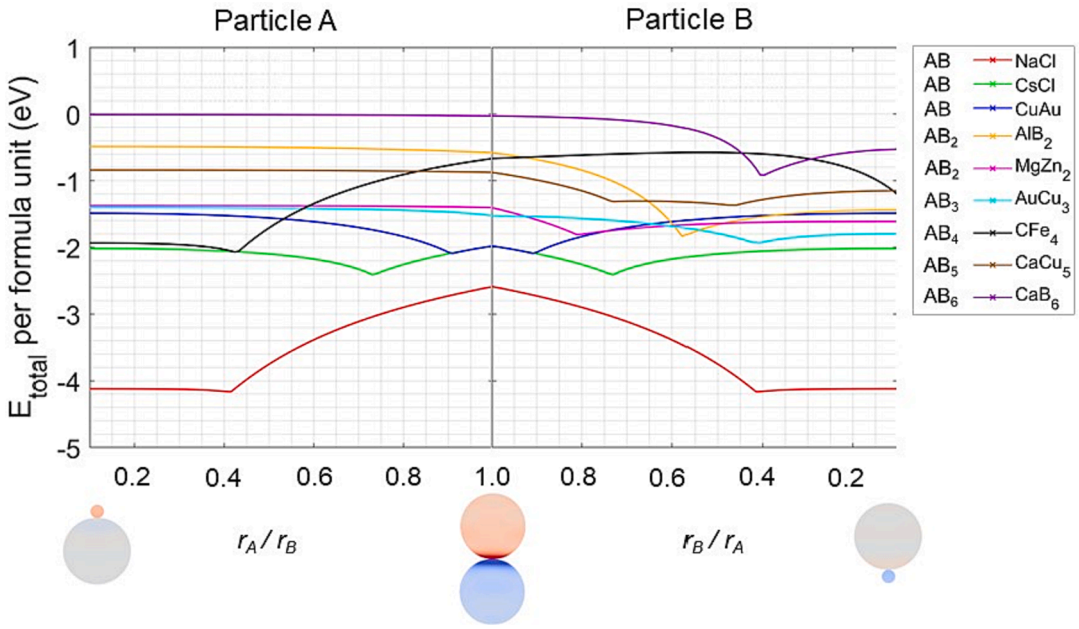

Fig. 2. Total electrostatic energy as a function of the radius ratio, γ, for all the lattice types under consideration. In the left-hand panel, particle A is reduced in size from 50 μm to 500 μm in diameter. In the right-hand panel, particle B is reduced in size over the same range.

Table 1
Values of the particle radius ratio (γ) calculated from minimum electrostatic energy configurations. These results are compared with available experimental data that have not necessarily been recorded for *charged* particles. The most stable ratio is shown in bold.

Lattice type	*γ (B/A)* (Min. elect. energy) Calculated	γ (Optimum packing) Experimental
NaCl	**0.42**	**0.41** [12]
CsCl	**0.73**	**0.73** [11]
CuAu	**0.91**	**1.0** [11]
AlB_2	**0.58**	**0.58** [11,12]
$MgZn_2$	**0.81**	**0.81** [11,12]
$AuCu_3$	**0.41** 1.0	**1.0** [11], 0.42 [11]
CFe_4	**0.42** [#]	
$CaCu_5$	**0.46**, 0.75	**0.65**, 0.75 [11]
CaB_6	**0.40**	**0.41** [37]

[#] Calculated for the ratio *γ (A/B)* corresponding to *r*(C)/*r*(Fe).

having the same amount of charge concentrated at a point at the centre of a particle. Thus, as long as each small particle remains at a fixed central position, the Coulomb energy, which corresponds solely to interactions between free charges on the particles, remains constant in the NaCl lattice for $\gamma \leq 0.41$, irrespective of the radius ratio across this range. In this rock-salt lattice, the radius ratio $\gamma = \sqrt{2}-1 \approx 0.41421\cdots$ equates to a perfect fit of a small particle inside an octahedral hole defined by larger particles. Even though such an assembly can still retain a negative interaction energy at small radius ratios, the structure could potentially be destabilised as each small particle becomes free to move inside an octahedral hole. As is clear from Fig. 4, the argument outlined above for NaCl is easily extended to all other lattice types since their Coulomb energy is also constant for values of γ less than a global energy minimum.

Fig. 5 shows the multipolar contributions to the stability of each lattice type and as noted above, these interactions are always attractive in vacuum, and therefore, make a negative contribution to the total

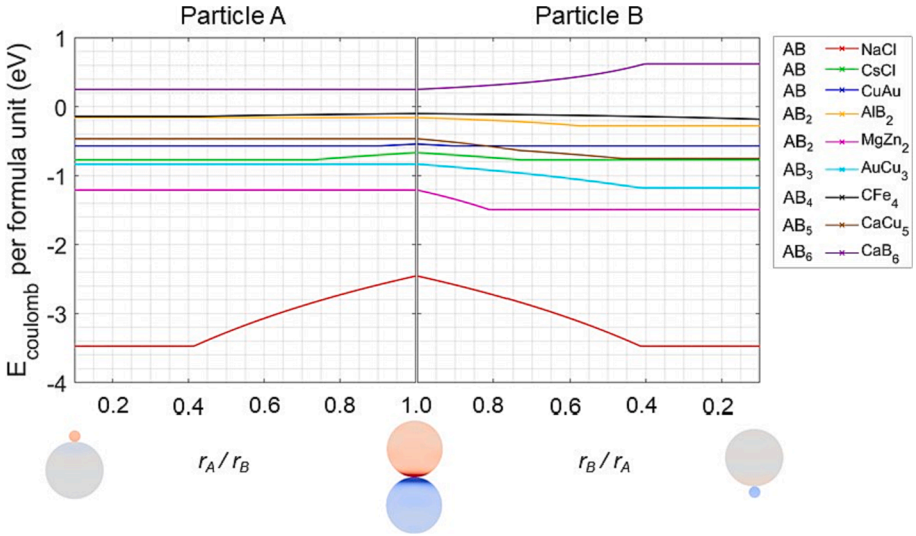

Fig. 3. As for Fig. 2, but a plot of the Coulomb energy as a function of γ.

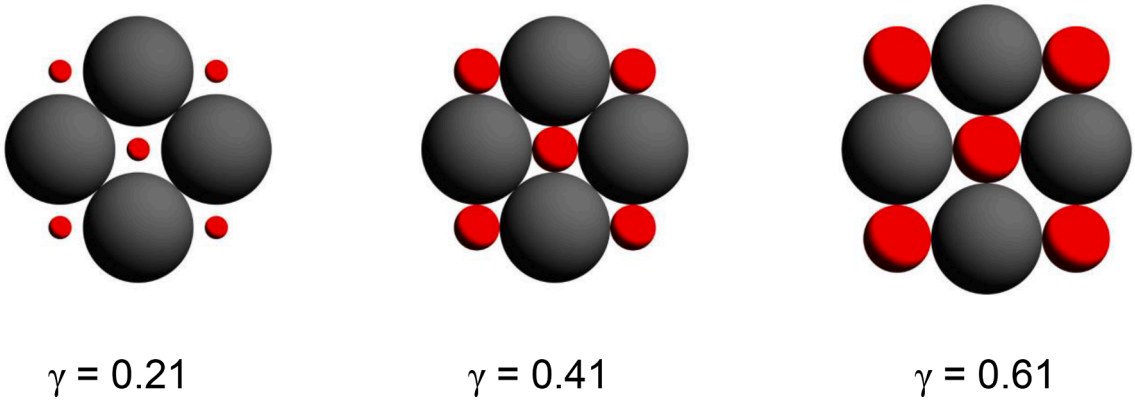

Fig. 4. Examples of the NaCl lattice type for different values of γ, the radius ratio.

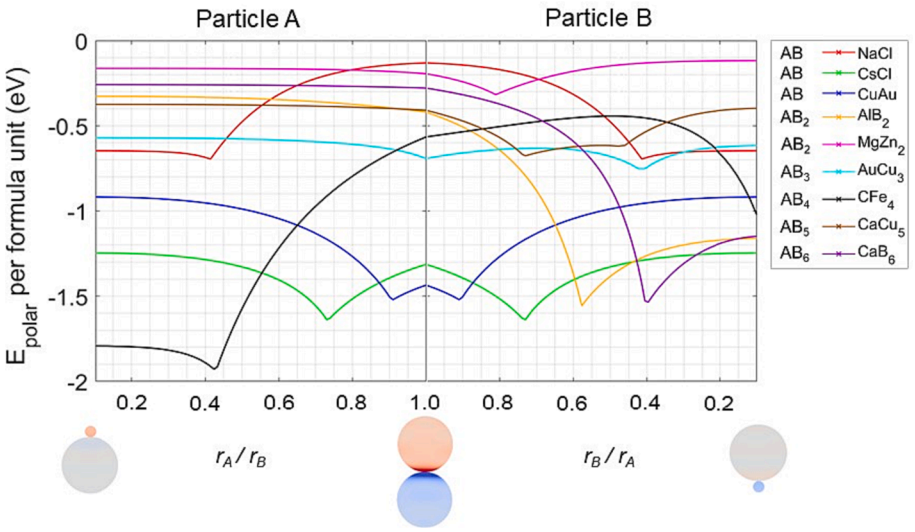

Fig. 5. As for Fig. 4, but a plot of the polarisation energy as a function of γ, the radius ratio.

electrostatic energy. What is clear from the results is that each lattice type shows one or more distinct energy minima in polarisation energy, and these coincide with the stable configurations identified in Fig. 2 and Table 1. Note that the total energy is given by the sum of the Coulomb and polarisation energies. Therefore, it would appear from comparisons between Figs. 2, 3 and 5, that for each of the γ values identified in Table 1 for a given lattice type, preferential stability is due entirely to multipolar interactions. Even for the NaCl lattice, true energy minima are only realised through the presence of multipolar contributions in the total electrostatic energy, and for the CaB_6 lattice type, multipolar interactions make the difference between stability and instability; this effect being over and above any entropic contribution to stability [37].

Two lattice types, $AuCu_3$ and $CaCu_5$ are calculated to exhibit both a local and a global energy minimum and similar observations have been made in experimental studies [11]; however, the calculated values for γ identified for global stable structures do not coincide with those seen by experiment [11]. The existence of two energy minima in lattices that are isostructural with $CaCu_5$, can be understood with the aid of Fig. 6. According to Fig. 2, a gradual increase in the size of the smaller particle (B) leads, in terms of the total energy, to a gradual increase in stability as gaps in the lattice become progressively filled, until the global energy minimum at $\gamma = 0.46$ is reached. As Fig. 6 shows, this value for γ corresponds to a structure where the surface of each particle touches an oppositely charged neighbour. As the size of the smaller particle increases beyond $\gamma = 0.46$, the energy initial increases very slightly before dropping to a new minimum at $\gamma = 0.73$. This latter configuration is determined by a maximum in the contribution from multipolar interactions to the total energy, as seen in Fig. 5. Whilst such a contribution, at approximately 50 % of the total energy, is significant, it is not large enough to shift the global minimum away from $\gamma = 0.46$. However, additional calculations show that a new global minimum at $\gamma = 0.73$ *would* appear if, instead of the complete many-body treatment presented here, the multipole contributions were computed as the sum of pair-wise interactions; this approach would lead to an over-estimation of the polarisation energy and promote a switch between minima. As γ increases beyond 0.73, the $CaCu_5$ lattice become less stable as gaps appear between particles and the multipolar contributions decrease in magnitude. As these results stand, any gain in attractive polarisation energy on the part of one particular geometry for $CaCu_5$, is conteracted by a decline in Coulomb energy. However, the very small difference in total energy (Fig. 2) between structures and the comparatively flat potential means that small changes in dielectric constant could easily lead to a switch in global stability. For $AuCu_3$ the circumstances surrounding the two stable structures are slightly different, in that the structure at $\gamma = 0.41$ is the more stable both in terms of Coulomb and many-body interactions. However, as Fig. 7 shows, stability of the $\gamma = 1.0$ structure, as favoured by experiment, relies on a higher percentage contribution from many-body interactions than when $\gamma = 0.41$; again therefore, a small change in dielectric constant could switch relative stabilities.

Fig. 7 shows the percentage contribution multipolar interactions make to the total energy, where it can be seen that for all but three lattice types, these contributions amount to over 50 % of the total energy and

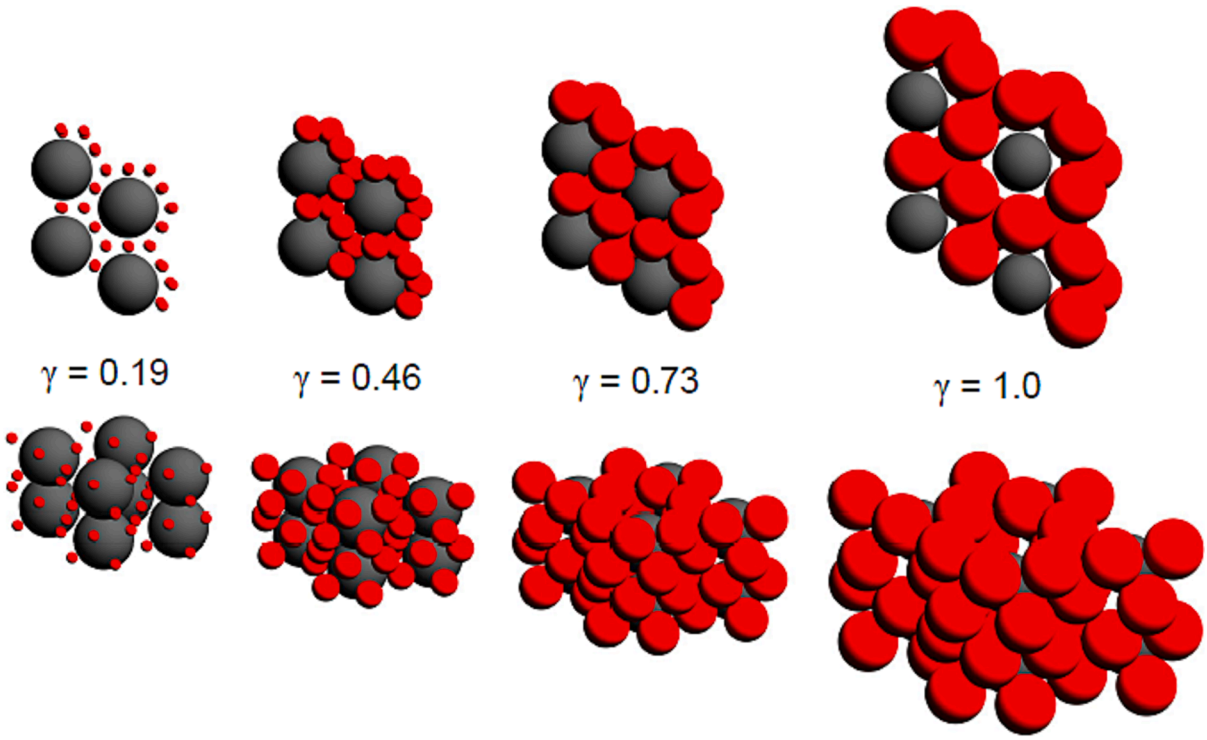

Fig. 6. Examples of the $CaCu_5$ lattice type for different values of γ, the radius ratio.

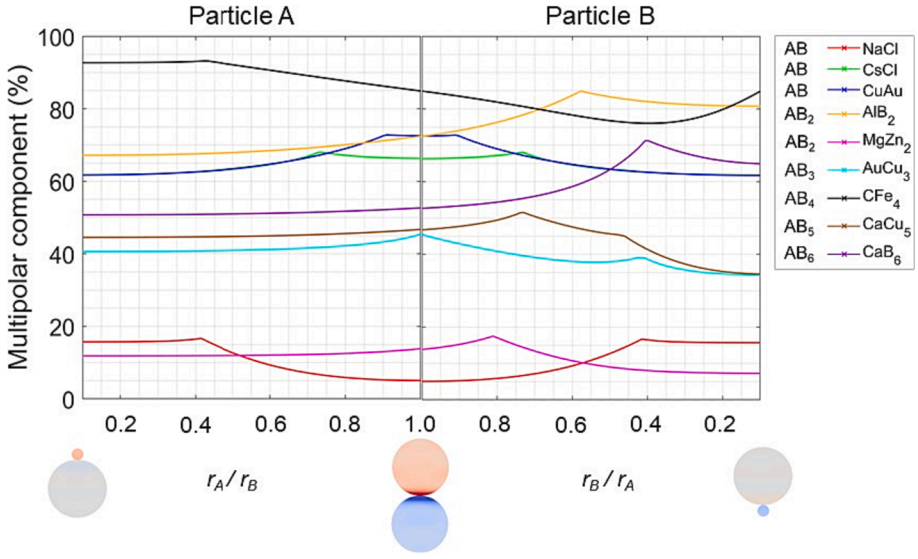

Fig. 7. As for Fig. 4, but showing the percentage contribtion from multipolar energy to the total electrostatic energy.

rising to ~95 % in the case of a CFe_4 lattice.

In many lattice structures of the type discussed above, the particles often consist of a solid core covered in surface ligands that form a capping layer [13,41]. Each particle then has an effective radius formed from the sum of two components, namely the core radius (r) and the length of the ligand (l) which together charaticterise a *softness* parameter, given by $s = l/r$. Typically, $s = 0.01$ for micron-sized particles, increasing to ~1 for nanoparticles [42]. Although ligands can contribute towards interactions between particles, more importantly, they mechanically prevent any direct contact between cores. Calculations with $s = 0.5$ show that, whilst the relative ordering of the strengths of the various interactions remains the same, the total electrostatic interaction energy can decrease by up to 50 %. However, for those lattice types that show a strong dependence on many-body interactions, for example Fe_4C and AlB_2, the percentage contribution of the latter to the total energy remains high.

3.3. Variation in dielectric constant

Thus far, all calculations have been undertaken with the particles having a dielectric constant of 20, which is taken to represent a mid point between polymer and metallic particles. In order to access the importance of the value assigned to k_i, further calculation have been undertaken where k_i has been given the values 2, 5, and 10. These results are summarised in Table 2 where, for each lattice type at the calculated global minimum, the percentage contribution from multipolar

Table 2
The effect changing the value of the dielectric constant has on the percentage contribution from multipolar interactions to the total energy. The symbol shown in bold is the small of the two different particles.

	Lattice type	Radius ratio γ	Multipolar contributions (%) at different values of the dielectric constant			
			$k_i = 2$	$k_i = 5$	$k_i = 10$	$k_i = 20$
AB	**Na**Cl	0.41	8	13	15	17
	CsCl	0.73	39	58	65	68
	CuAu	0.91	45	64	70	73
AB_2	Al$\mathbf{B}_2$	0.58	66	80	83	85
	Mg$\mathbf{Zn}_2$	0.81	8	14	16	18
AB_3	Au$\mathbf{Cu}_3$	0.41	16	30	36	39
AB_4	$\mathbf{C}Fe_4$	0.42	82	90	92	93
AB_5	Ca$\mathbf{Cu}_5$	0.46	21	36	42	45
AB_6	Ca$\mathbf{B}_6$	0.41	45	63	69	71

interactions is given for each value of the dielectric constant. The results for $k_i = 20$ are also given for comparison. As seen from the table, the largest differences occur when the dielectric constants are small and the reason for this can be seen from expanded expressions for the force between particles [28], where the dielectric constant frequently appears in the form of a ratio: $(k_i - 1)/(k_i + 2)$, which varies from 0.25 when $k_i = 2$ to 0.57 at $k_i = 5$ and 0.86 when $k_i = 20$. However, it is also clear from Table 2 and Fig. 5 that for certain lattice types, for example, AB_2 and AB_4 the dielectric constant, irrespective of its value, has a strong influence on the magnitude of the electrostatic interaction. For other lattice types, for example those of NaCl and $MgZn_2$, many-body contributions are only ever going to be small at any value assigned to k_i. For an NaCl-type lattice consisting of colloidal particles and embedded point charges, Barros *et al.* [21] have shown that a change in dielectric constant can lead to a structural change; such behaviour has not been explored in these calculations.

4. Conclusion

A new development in the theory of charge-induced, many-body electrostatic interactions has made it possible to investigate the extent to which such forces may be responsible for the fabrication and structural stability of seven frequently observed binary, particulate lattice structures. The calculations show that, for lattices arrays known to involve charged particles, between 15 % and 90 % of the lattice energy could be derived from effects due to many-body electrostatic polarisation. The non-additive influence of polarisation, as opposed to pair-wise interactions, is also shown to be necessary in order to distinguish true from local energy minima. For a lattice isostructural with CFe_4, a particle size ratio not previously observed is found to be particularly stable due to many-body effects.

CRediT authorship contribution statement

Eric B. Lindgren: Formal analysis, Investigation, Methodology, Software, Writing – original draft, Writing – review & editing. **Holly Avis:** Data curation, Formal analysis, Investigation. **Abigail Miller:** Data curation, Formal analysis, Investigation. **Benjamin Stamm:** Formal analysis, Investigation, Methodology, Software, Supervision, Writing – original draft, Writing – review & editing. **Elena Besley:** Formal analysis, Funding acquisition, Investigation, Methodology, Supervision, Writing – original draft, Writing – review & editing. **Anthony J. Stace:** Conceptualization, Formal analysis, Investigation, Supervision, Writing – original draft, Writing – review & editing.

Declaration of competing interest

The authors declare the following financial interests/personal relationships which may be considered as potential competing interests: Anthony Stace reports financial support was provided by Leverhulme Trust. Elena Besley reports financial support was provided by The Royal Society. Abigail Miller reports financial support was provided by Engineering and Physical Sciences Research Council. If there are other authors, they declare that they have no known competing financial interests or personal relationships that could have appeared to influence the work reported in this paper.

Data availability

Data will be made available on request.

Acknowledgements

The authors would like to thank the International Space Science Institute (Bern) for supporting this collaboration. EB acknowledges financial support from a Royal Society Wolfson Fellowship. AJS would like to thank the Leverhulme Trust for the award of an Emeritus Fellowship.

References

[1] J.S. Méndez-Harper, G.D. McDonald, J. Dufek, M.J. Maslaska, D.M. Burr, A. G. Hayes, J. McAdams, J.J. Wray, Electrification of sand on Titan and its influence on sediment transport, Nat. Geosci. 10 (2017) 260–265.
[2] S. Okuzumi, Electric charging of dust aggregates and its effect on dust coasgulation in protoplanetary disks, ApJ 698 (2009) 1122–1135.
[3] T. Steinpilz, K. Joeris, F. Jungmann, D. Wolf, L. Brendel, J. Teiser, T. Shinbrot, G. Wurm, Electrical charging overcomes the bouncing barrier in planet formation, Nat. Phys. 16 (2020) 225–229.
[4] V. Lee, S.R. Waitukaitis, M.Z. Miskin, H.M. Jaeger, Direct observation of particle interactionsd and clustering in charged granular streams, Nat. Phys. 11 (2015) 733–737.
[5] J. Méndez-Harper, J. Dufek, The effects of dynamics on the triboelectrification of volcanic ash, J. Geophys. Res. Atmos. 121 (2016) 8209–8228.
[6] H. Lee, S. You, P.V. Pikhitsa, J. Kim, S. Kwon, C.G. Woo, M. Choi, Three-dimensional assembly of nanoparticles from charged aserosols, Nano Lett. 11 (2011) 119–124.
[7] B. Grzybowski, A. Winkleman, J.A. Wiles, Y. Brumer, G.M. Whitesides, Electrostatic self-assembly of macroscopic crystals using contact electrification, Nat. Mater. 2 (2003) 241–245.
[8] R. Cademartiri, C.A. Stan, V.M. Tran, E. Wu, L. Friar, D. Vulis, L.W. Clark, S. Tricard, G.M. Whitesides, A simple two-dimensional model system to study electrostatic-self-assembly, Soft Matter 8 (2012) 9771–9791.
[9] E.B. Lindgren, B. Stamm, Y. Maday, E. Besley, A.J. Stace, Dynamic simulations of many-body electrostatic self-assembly, Phil. Trans. R. Soc. A 376 (2018) 20170143.
[10] J. Haeberie, J. Harju, M. Sperl, P. Born, Granular ionic crystals in a small nutshell, Soft Matter 15 (2019) 7179–7186.
[11] M.I. Bodnarchuk, M.V. Kovalenko, W. Heiss, D.V. Talapin, Energetic and entropic contributions to self-assembly of binary nanocrystal supperlattices: temperature as the structure-directing factor, J. Am. Chem. Soc. 132 (2010) 11967–11977.
[12] E.V. Shevchenko, D.V. Talapin, C.B. Murray, S. O'Brien, Structural characterization of self-assembled multifunctional binary nanoparticle superlattices, J. Am. Chem. Soc. 128 (2006) 3620–3637.
[13] E.V. Shevchenko, D.V. Talapin, N.A. Kotov, S. O'Brien, C.B. Murray, Structural diversity in binary nanoparticle superlattices, Nature 439 (2006) 55–59.
[14] E.B. Lindgren, A.J. Stace, E. Polack, Y. Maday, B. Stamm, E. Besley, An integral equation approach to calculate electrostatic interactions in many-body dielectric systems, J. Comp. Phys. 371 (2018) 712–731.
[15] M.E. Leunissen, C.G. Christova, A.-P. Hynninen, C.P. Royall, A.I. Campbell, A. Imhof, M. Dijkstra, R. van Roij, A. van Blaaderen, Ionic colloidal crystals of oppositely charged particles, Nature 437 (2005) 235–240.
[16] D.V. Talapin, E.V. Shevchenko, C.B. Murray, A.V. Titov, P. Král, Dipole-dipole interactions in nanoparticle superlattices, Nano Lett. 7 (2007) 1213–1219.
[17] A. Ben-Simon, H. Eshet, E. Rabani, On the phase behavior of binary mixtures of nanoparticles, ACS Nano 7 (2013) 978–986.
[18] M.I. Bodnarchuk, R. Erni, F. Krumeich, M.V. Kovalenko, Binary superlattices from colloidal nanocrystals and giant polyoxometalare clusters, Nano Letts. 13 (2013) 1699–1705.
[19] A.F. Demirörs, J.C.P. Stiefelhagen, T. Vissers, F. Smallenburg, M. Dijkstra, A. Imhof, A. van Blaaderen, Long-ranged oppositely charged interactions for designing new types of colloidal clusters, Phys. Rev. X 5 (2015) 021012.
[20] K. Barros, D. Sinkovits, E. Luijten, Efficient and accurate simulations of dynamic dielectric objects, J. Chem. Phys. 140 (2014) 064903.
[21] K. Barros, E. Luijten, Dielectric effects in the self-assembly of binary colloidal aggragates, Phys. Rev. Letts. 113 (2014) 017801.
[22] J. Qin, J.J. de Pablo, K.F. Freed, Image method for induced surface charge from many-body system of dielectric spheres, J. Chem. Phys. 145 (2016) 124903.

[23] J. Qin, J. Li, V. Lee, H. Jaeger, J.J. de Pablo, K.F. Freed, A theory of interactions between polarizable dielectric spheres, J. Coll. Interf. Sci. 469 (2016) 237–241.
[24] J. Qin, Charge polarization near dielectric interfaces and the multiple-scattering formalism, Soft Matter 15 (2019) 2125–2134.
[25] M. Hassan, B. Stamm, An integral equation formulation of the N-body dielectric spheres problem Part I: numerical analysis, ESAIM: Math. Modell. Numer. Anal. 55 (2021) S65–S102.
[26] B. Bramas, M. Hassan, B. Stamm, An integral equation formulation of the N-body dielectric spheres problem Part II: complexity analysis, ESAIM: Math. Modell. Numer. Anal. 55 (2021) 5625–5651.
[27] M. Hassan, B. Stamm, A linear scaling in accuracy numerical method for computing the electrostatic forces in the N-body dielectric sphere problem, Commun. Comput. Phys. 29 (2021) 319–356.
[28] E. Bichoutskaia (Besley), A.L. Boatwright, A. Khachatourian, A.J. Stace, Electrostatic analysis of the interactions between charged particles of dielectric materials, J. Chem. Phys. 133 (2010) 024105.
[29] L. Greengard, V. Rokhlin, A fast algorithm for particle simulations, J. Comp. Phys. 73 (1987) 325–348.
[30] A.J. Stone, The theory of Intermolecular Forces, 2nd ed., OUP, Oxford, 2013.
[31] F.N. Mehr, D. Grigoriev, R. Heaton, J. Baptiste, A.J. Stace, N. Puretskiy, E. Besley, A. Böker, Self-assembly behavior of oppositely charged inverse bipatchy microcolloids, Small 16 (2020) 2000442.
[32] A.V. Filipov, X. Chen, C. Harris, A.J. Stace, E. Besley, Interactions between particles with inhomogeneous surface charge distributions: revisiting the Coulomb fission of dication molecular clusters, J. Chem. Phys. 151 (2019) 154113.
[33] A.J. Stace, A.L. Boatwright, A. Khachatourian, E. Bichoutskaia, Why like-charged particles of dielectric materials can be attracted to one another, J. Coll. Interface Sci. 354 (2011) 417–420.
[34] E.B. Lingren, Q. Chaoyu, B. Stamm, Theoretical analysis of screened many-body electrostatic interactions between charged polarizable particles, J. Chem. Phys. 150 (2019) 044901.
[35] I.N. Derbenev, A.V. Flippov, A.J. Stace, E. Besley, Electrostatic interactions between charged dielectric particles in an electrolyte solution: constant potential boundary conditions, Soft Matter 14 (2018) 5480–5487.
[36] I. Lotan, T. Head-Gordon, An analytical electrostatic model for salt screened interactions between multiple proteins, J. Chem. Theory Comp. 2 (2006) 541–555.
[37] X. Ye, J. Chen, C.B. Murray, Polymorphism in self-assembled AB(6) binary nanocrystal superlattices, J. Am. Chem. Soc. 133 (2011) 2613–2620.
[38] A. Jain, S.P. Ong, G. Hautier, W. Chen, W.D. Richards, S. Dacek, S. Cholia, D. Gunter, D. Skinner, G. Ceder, K. Persson, Commentary: The Materials Project: a materials genome approach to accelerating materials innovation, APL Mater. 1 (2013) 011002.
[39] M.D. Hanwell, D.E. Curtis, D.C. Lonie, T. Vandermeersch, E. Zurek, G.R. Hutchison, Avogadro: an advanced semantic chemical editor, visualization, and analysis platform, J. Cheminformatics 4 (2012) 17.
[40] E.B. Lindgren, I.N. Derbenev, A. Khachatourian, H.-K. Chan, A.J. Stace, E. Besley, Electrostatic self-assembly: understanding the significance of the solvent, J. Chem. Theory Comput. 14 (2018) 905–915.
[41] M.V. Kovalenko, L. Manna, A. Cabot, Z. Hens, D.V. Talapin, C.R. Kagan, V. I. Klimov, A.L. Rogach, P. Reiss, D.J. Milliron, P. Guyot-Sionnnest, G. Konstantatos, W.J. Parak, T. Hyeon, B.A. Korgel, C.B. Murray, W. Heiss, Prospects of nanoscience with nanocrystals, ACS Nano 9 (2015) 1012–1057.
[42] M.A. Boles, D.V. Talapin, Many-body effects in nanocrystal superlattices: departure from sphere packing explains stability of binary phases, J. Am. Chem. Soc. 137 (2015) 4494–4502.